Near-resonant propagation of short pulses in a two-level medium

Xiang-yang Yu,* Wei Liu, and Cheng Li
State Key Laboratory of Optoelectronic Materials and Technologies, Sun Yat-Sen University, Guangzhou 510275, China
(Received 3 July 2010; published 9 September 2011)

We present a numerical method for solving the Maxwell-Bloch equations describing pulse propagation for a two-level medium. The method is accurate, efficient, stable, and well suited for this type of simultaneous equations. By applying the numerical scheme we investigate the evolutions of pulse area, pulse propagation, pulse velocity, and spectral shapes under both homogeneous and inhomogeneous broadening conditions. The results show that the area evolution and pulse-reshaping procedure are significantly influenced by detuning and inhomogeneous line shape, which also impact the oscillation tail and pulse peak. In addition, the pulse-peak traces indicated the pulse velocity always increases with greater deviation in pulse-area value from the value 2π. We also demonstrate the pulse velocity increased for a larger detuning or a wider inhomogeneous line shape. Furthermore, the spectral feature shows that pulse spectra evolve into an oscillating shape.

DOI: 10.1103/PhysRevA.84.033811 PACS number(s): 42.50.Ct, 42.65.Re

I. INTRODUCTION

The coherent interaction of ultrashort optical pulses with resonant medium is a fundamental problem in quantum optics [1]. The recent advance in ultrafast laser technology has made it possible to generate extremely short and intense pulses, such as single attosecond [2,3] pulses. It has attracted much interest in the interaction of ultrashort pulse and atoms all over the world. In the ultrafast regime, frequently in femtoseconds, the relaxation has insufficient time to destroy the coherence, which makes the phenomenon of light-matter interaction become very interesting in such transient coherent processes.

On the condition that atomic relaxation is neglected, the famous area theorem [4] governs the coherent nonlinear transmission of ultrashort optical pulses through an inhomogeneously broadened medium which has an absorption resonance frequency. Even the profile of few-cycle pulse evolution can still be predicted by the area theorem [5]. A derivation of the area theorem including pulse chirping is also obtained and can be used to investigate pulse phase evolution [6]. In most theoretical analyses for pulses at the subfemtosecond level, the effects of the relaxation of the atomic system are neglected since the durations of the pulses are far smaller than the decay time. While considering the relaxation time, the effects of the relaxation rate on pulse-area evolution have been extensively investigated [7], which shows numerically that the stabilization of the pulse area is not permanent because the energy losses are due to the spontaneous decay. By zero-area pulse [8], in the cases of both off resonance and on resonance, zero-area pulse can produce complete population transfer in a two-state quantum system [9]. As to the near-resonant case, it also presents that the generalized pulse area is stabilized for relatively small detunings [10]. For the phase of ultrashort pulses in two-level systems, the measurement of the pulse phase has been studied in theory and experiment [11,12]. As to the spectral evolution in the atomic system, many studies are devoted to the spectral modifications [13], and the spectral feature appears to be transition frequency and has significant deviation from a simple Lorentzian dip for a larger pulse area [14,15]. The changes in the spectrum of a near-resonant pulse propagating through a two-level atomic system have also been theoretically and experimentally studied [16]. It was shown that at the transition frequency the spectrum structure of the transmitted pulse depends sensitively on the pulse area, the pulse detuning, and the absorption path length. Pulse shape is a visual display of pulse evolution in a medium. It is reported that by using a strong off-resonant ultrashort pulse one can control the shape of a weak, resonant, ultrashort pulse propagating in an assembly of two-level atoms [17]. Actually, without the driven pulse, the propagation of ultrashort laser pulses in a resonant atomic medium can lead to strong reshaping effects by dispersion [1,18].

Despite the above extensive work, in comparison, only a few theoretical or experimental studies [17] have been devoted to the influence of the absorption spectral bandwidth on the pulse shape, the pulse velocity, the pulse spectrum, and other pulse-propagation properties. The inhomogeneous linewidth [1] of a medium characterizes the absorption spectral bandwidth. A large inhomogeneous linewidth means a strong inhomogeneous broadening effect, and the carrier frequency is included in absorption line. In the opposite case, the absorption spectral bandwidth is very narrow and dominates closely around the central frequency (and even can be represented by the δ function). In this paper, we establish a powerful numerical scheme to simulate the light-matter interaction in a two-level medium. By applying this accurate and effective numerical procedure, we analyze the evolution of pulse area in the case of nonzero detuning for different inhomogeneous linewidths. To have a further understanding of the interaction of coherent pulses with the medium, an extended study of the behaviors of pulse shape and velocity during propagation in a two-level medium was performed. With all these effects in mind we restrict our attention to the resonant and near-resonant interaction and focus on the basic two-level system.

This paper is organized as follows. In Sec. II the basic equations and definitions are introduced. Sec. III elaborates the numerical procedure and gives the flow chart. Sec. IV is devoted to a numerical analysis of the behaviors of the generalized pulse area and pulse-propagation properties and discusses the influence of pulse and medium parameters on

*cesyxy@mail.sysu.edu.cn

the pulse velocity and spectral shapes. Finally, in Sec. V we present our conclusions.

II. BASIC EQUATIONS AND DEFINITIONS

To study pulse propagation we solve the simultaneous Maxwell-Bloch equations for a two-level medium with the rotating-wave approximation and consider the propagation in the direction z. The Maxwell equation for propagation is

$$\dot{\Omega}_t(z,t) + cn^{-1}\dot{\Omega}_z(z,t) = \tau_0^{-2}\int_{-\infty}^{\infty} v \cdot g(\Delta)d\Delta, \tag{1}$$

where $\tau_0 = (2\hbar n^2/N\mu_0 c^2\mu^2\omega)^{1/2}$ is the effective time, $\Delta = \Delta_0 + \omega - \omega_0$ is the detuning of the laser frequency ω from the resonance frequency ω_0, Δ_0 is caused by inhomogeneous broadening, $g(\Delta)$is the absorption line shape, such as the line shape determined by Doppler broadening, N is the atomic density, n is the medium's refractive index, $\Omega(z,t) = \mu\tilde{E}(z,t)/\hbar$ is the Rabi frequency, $\tilde{E}(z,t)$ is the field envelope of the pulse, and $v(\Delta,z,t)$ is the component of the Bloch vector that determines the absorption of a single atom and can be calculated from the Bloch equations

$$\begin{aligned} \dot{u}_t &= -u/T_2 - \Delta \cdot v \\ \dot{v}_t &= -v/T_2 + \Delta \cdot u + \Omega \cdot w \\ \dot{w}_t &= -(w - w_0)/T_1 - \Omega \cdot v. \end{aligned} \tag{2}$$

Here w_0 is the initial population difference between the upper and lower states and T_1 and T_2 are the longitudinal and transverse relaxation times, respectively. Dimensionless space and time variables are $z' = nz/c\tau_0$, $t' = t/\tau_0$, $T_1' = T_1/\tau_0$, $T_2' = T_2/\tau_0$, $\Omega' = \Omega\tau_0$, and $\Delta' = \Delta\tau_0$. For convenience, we record z',t',T_1',T_2',Ω', and Δ' as z,t,T_1,T_2,Ω, and Δ. Equations (2) are unchanged, but Eq. (1) is reduced to

$$\dot{\Omega}_t(z,t) + \dot{\Omega}_z(z,t) = \int_{-\infty}^{\infty} v \cdot g(\Delta)d\Delta. \tag{3a}$$

In Eq. (3a), $g(\Delta)$ is the normalized inhomogeneous line shape. Before going further, we point out that in homogeneously broadened medium, $g(\Delta)$ is too narrow to have an effect on the integral term, and it is written

$$\dot{\Omega}_t(z,t) + \dot{\Omega}_z(z,t) = v(z,t). \tag{3b}$$

We define it as a Gaussian line shape function

$$g(\Delta) = \sqrt{2\ln 2/\pi\,\Delta_d^2}\,e^{-\frac{2\ln 2}{\Delta_d^2}\Delta^2}, \tag{4}$$

where Δ_d is the full width at half maximum of the inhomogeneous line shape (FWHM ILS). The simultaneous solution of Eqs. (2) and (3) leads to fields that, when they are integrated over time at each propagation distance, give the area

$$S(z) = \int_{-\infty}^{\infty} \Omega(z,t')dt', \tag{5}$$

which obeys the simple equation [2]

$$\frac{dS}{dz} = -\frac{\alpha}{2}\sin S, \tag{6}$$

where $\alpha = \omega\pi\mu_0 N\mu^2 c g(0)/n\hbar$ is the linear optical attenuation coefficient for the material and $g(0)$ is a Gaussian line shape with its maximum at $\Delta = 0$. It proves useful to define Ω as follows:

$$\Omega(t) = \Omega_0 e^{-\frac{2\ln 2}{t_p^2}t^2}, \tag{7}$$

where t_p is the FWHM of the Gaussian pulse and Ω_0 is the pulse peak. Fourier transform solution of Eq. (7) shows the spectrum FWHM of the input pulse is $\Delta_p = 2\sqrt{2}\ln 2/(\pi t_p)$.

III. NUMERICAL PROCEDURE

Because, in general, the set of coupled Eqs. (2) and (3) cannot be solved analytically, numerical computations are necessary. In this section we describe the method of predictor-corrector fourth-order Runge-Kutta scheme that we used to calculate the dynamical properties of Maxwell-Bloch equations. Our computational procedure includes the initial value predictor cycle and the corrector-predictor cycle. As we mentioned above, our method is designed to simulate wave propagation through a two-level medium. Since the emphasis here is on the numerical procedure, we show just the particular set of the coupled Eqs. (2) and (3).

In practice it is often useful for Eqs. (2), dependent on the time differential only, to be solved by using the classical fourth-order Runge-Kutta scheme. This procedure is discussed in more detail in [15]. The method we use can be written as

$$\begin{aligned} u_{t+1} &= u_t + h_t(f_{u1} + 2f_{u2} + 2f_{u3} + f_{u4})/6, \\ v_{t+1} &= v_t + h_t(f_{v1} + 2f_{v2} + 2f_{v3} + f_{v4})/6, \\ w_{t+1} &= w_t + h_t(f_{w1} + 2f_{w2} + 2f_{w3} + f_{w4})/6, \end{aligned} \tag{8}$$

where h_t is the step size for differentiation in time domain and f_{ui}, f_{vi}, and f_{wi} are the right-hand sides of Eqs. (2), respectively. As illustrated in Fig. 1(a), $m = T/h_t$, where T is the time length. Equation (3) has the important property that its characteristics depend on both the space differential and the time differential. We first consider the right-hand side of Eq. (3a). The integral term is a cumulative sum of

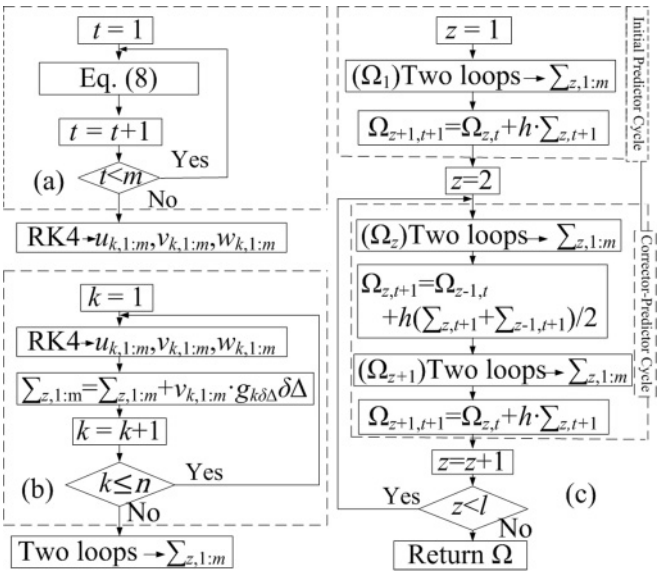

FIG. 1. Flow charts for subroutines of (a) partial differential Bloch equations and (b) integral equations. (c) Main routine flow chart.

inhomogeneous line shape [Fig. 1(b)] and can be rewritten in integral form as

$$\int_{-\infty}^{\infty} v(\Delta,z,t)\cdot g(\Delta)d\Delta = \sum_{k} v(k\delta\Delta,z,t)\cdot g(k\delta\Delta)\delta\Delta, \quad (9)$$

where $\delta\Delta$ is the step size of inhomogeneous line shape. For convenience, we record the right side of Eq. (9) as $\Sigma_{z,t}$[in a homogeneous broadened medium, Eq. (9) is neglected and $\Sigma_{z,t} = v(z,t)$]. The simple finite-difference form of Eq. (3) is

$$(\Omega_{z+1,t+1} - \Omega_{z,t+1})/h_z + (\Omega_{z,t+1} - \Omega_{z,t})/h_t = \sum_{z,t+1}. \quad (10)$$

where h_z is the distance between any two space neighboring points. We assume the step size for differentiation in time is the same as the step size for differentiation in space for simplicity, which is $h = h_z = h_t$. Hence, it can be viewed as a rectangle in z and t space with a square mesh of points. Equation (10) is reduced to

$$\Omega_{z+1,t+1} = \Omega_{z,t} + h\sum_{z,t+1}. \quad (11)$$

In order to enhance the numerical calculation accuracy, we use the middle grid point to improve the simple finite-difference scheme. Thus

$$\Omega_{z+1,t+1} = \Omega_{z,t} + h\left(\sum_{z,t+1} + \sum_{z+1,t+1}\right)/2. \quad (12)$$

In order to solve the coupled Eqs. (2) and (3), we apply a predictor-corrector scheme. To understand this technique, we first look at *the initial value predictor cycle*; the envelope function of the Rabi frequency is given by Eq. (7). In addition, we assume that the system initially contains no energy, which means $u_0 = 0$, $v_0 = 0$, and $w_0 = -1$ (all atoms at the ground state). We obtain u, v, and w by applying the classical fourth-order Runge-Kutta scheme under the determined value Δ and $z = 1$, then integrate u using Eq. (9) under the determined value $z = 1$ when starting at $\Delta = -\infty$ and ending at $\Delta = \infty$, and finally substitute Σ_1 into Eq. (11) to obtain the next Ω ($z = 2$) in the time domain, as we show in Fig. 1(c).

During *the corrector-predictor cycle*, again using the fourth-order Runge-Kutta scheme and integrating the Eq. (9), we then substitute Σ_{z-1} and Σ_z into Eq. (12) to obtain the corrected Ω_z. We note that the corrected Ω_z should be used to correct u, v, and w under the value z. Again we substitute the obtained u into Eq. (9) to get the integrating value Σ_{z+1}, and we have the predictor value Ω_{z+1}. As illustrated in Fig. 1(c), our program loop returns to the starting point of the corrector-predictor cycle under the condition of $z < l$ ($l = L/h$, where L is the length).

We point out again that, under the condition of a homogeneously broadened medium, the subroutine of the integral equations in the main routine flow chart shown in Fig. 1(c) is neglected and replaced by the subroutine of partial differential Bloch equations. So *the initial value predictor cycle* and *the predictor-corrector cycle* no longer need to apply the integral procedure; other procedures are the same as described above.

The numerical procedure is now clear. In the way described above, we finally obtain the value of ω describing the desired signal and the evolution of Bloch vectors in both homogeneously and inhomogeneously broadened media. Our method, compared with the finite-difference method or a general numerical scheme, has the advantage that it needs far less calculation time (three or two orders of magnitude lower) for the same accuracy, [19,20], which is discussed in the Appendix.

IV. RESULTS AND DISCUSSION

Now we apply the numerical procedure to investigate the behavior of the pulse propagation in a two-level medium. In the calculations relative units of time τ_0 and distance $c\tau_0/n$ are used, and all other parameters are also given in relation to the scaled time τ_0 (see Sec. II).

A. Pulse area

Here we present a numerical analysis of the pulse area in homogeneously and inhomogeneously broadened two-level media. We begin from the analysis of the behavior of the pulse area (according to Eq. (5), the definition pulse area is a time integral starting at $-\infty$ and ending at ∞) during propagation. In the area theorem [1], it is obtained that the evolution of the pulse area depends on the input pulse area and the linear optical attenuation coefficient for the material, and there are two striking consequences of the area theorem, which are (i) pulses with special values of area, namely, integer even multiples of π, will not change the pulse area but will finally split into multiple 2π pulses and (ii) a pulse area with other values is predicted to reshape into integer even multiples of π value and also evolve into multiple 2π pulses [1,6]. Those properties can be shown to be stable in an inhomogeneously broadened medium if the atomic relaxation is neglected.

The area theorem is not suitable for a homogeneously broadened medium, as presented in Fig. 2(a), in which we have plotted the area S as a function of distance for different input areas of the pulse. We restrict our calculations to the resonant and ultrashort pulses, and the time duration of the input pulse

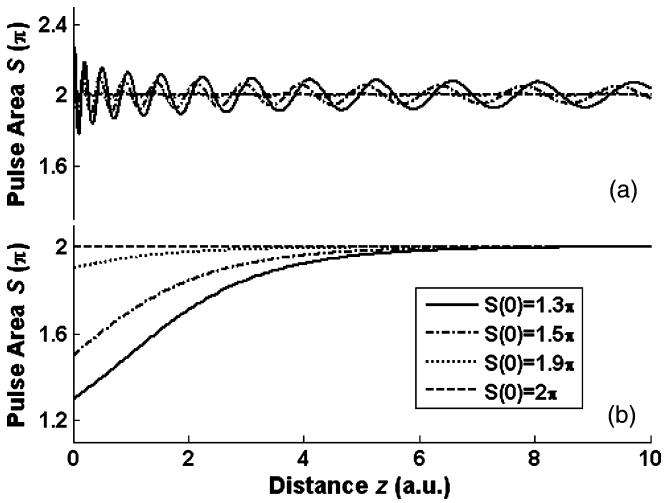

FIG. 2. The spatial evolution of pulse area for four values of the input pulse area in (a) homogeneously and (b) inhomogeneously broadened media.

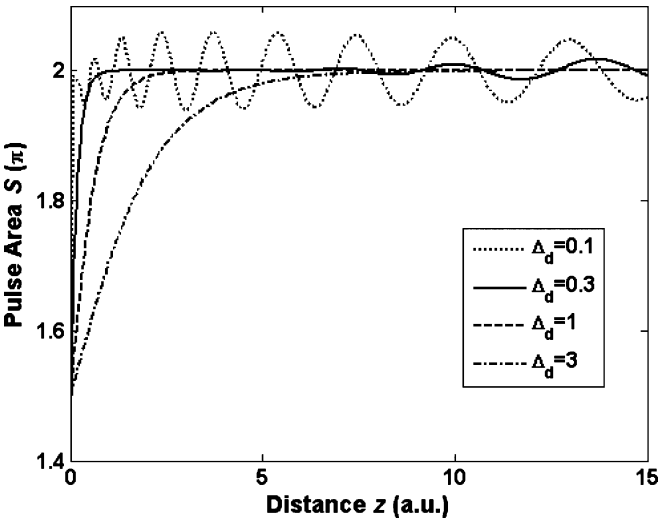

FIG. 3. Evolution of pulse area as a function of propagation distance for different FWHM ILS.

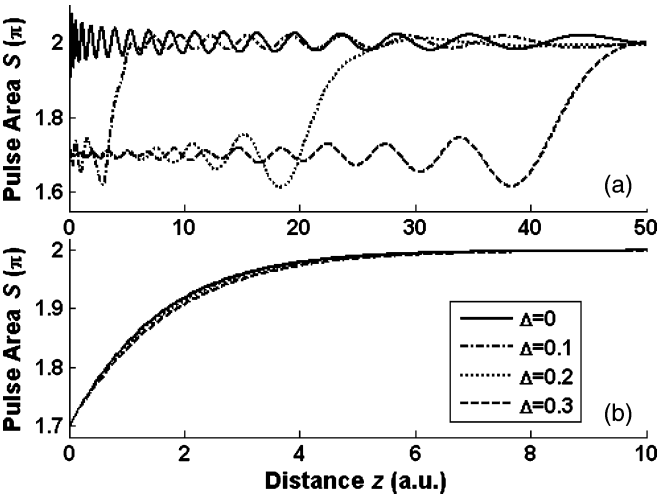

FIG. 5. Pulse area as a function of distance for different detuning values in (a) homogeneously and (b) inhomogeneously broadened media.

is neglected. It is obvious that the formed oscillation and its properties should strongly depend on the initial pulse area. To show this feature of the propagation we have analyzed the pulse behavior with different initial areas. Fig. 2(a) shows that the pulse with $S(0) = 1.3\pi$ needs a very short distance (almost $z = 0.02$) to approach 2π and then oscillates around the value 2π. The continuous oscillation amplitude becomes smaller as distance increases, and the oscillation period, as a function of the distance, becomes longer with the increasing of distance. As compared with the pulses having areas of 1.5π and 1.9π, the pulse with a larger area needs a shorter distance to approach 2π, and the oscillation period and amplitude are also decreased relatively. While the initial input pulse area is 2π, the pulse area remains unchanged and without oscillation; actually, the shape and peak amplitude of the pulse are stable as it propagates through the medium.

The presence of our numerical calculations in Fig. 2(b) shows that the smaller the initial pulse area is, the longer the optical path needed to approach 2π is. Exactly, it proves that the area evolution in an inhomogeneously broadened medium strictly obeys the area theorem in the absence of relaxation time.

One of the most interesting results of the area evolution in a medium is the effect of the inhomogeneous line shape. Here we give a few results showing the influence of the FWHM ILS Δ_d, which characterizes the inhomogeneous line shapes $g(\Delta)$ on this effect. Figure 3 shows the process of a pulse in resonance and with an input area $S(0) = 1.5\pi$ converting into a 2π pulse. In general, for a relatively large value of $\Delta_d(=3)$, the evolution curve of the pulse area to approach 2π is smooth. As to the value of $\Delta_d = 0.3$, the distance of the 1.5π pulse approaching to 2π is relatively shortened, and an oscillation tail appears. Decreasing Δ_d (such as the dotted curve in Fig. 3) results in the shortening of the approaching distance and makes the oscillation increasingly stronger. Compared with the area evolution in Fig. 2(a), we find out that the smaller the value of Δ_d is, the closer the evolution properties are. Actually, homogeneous broadening is the limit of Δ_d as it tends to zero [1].

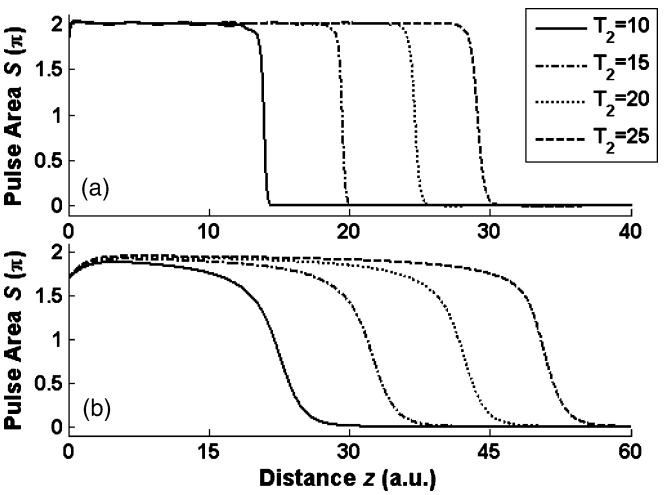

FIG. 4. The spatial evolution of pulse area for different relaxation times in (a) homogeneously and (b) inhomogeneously broadened media.

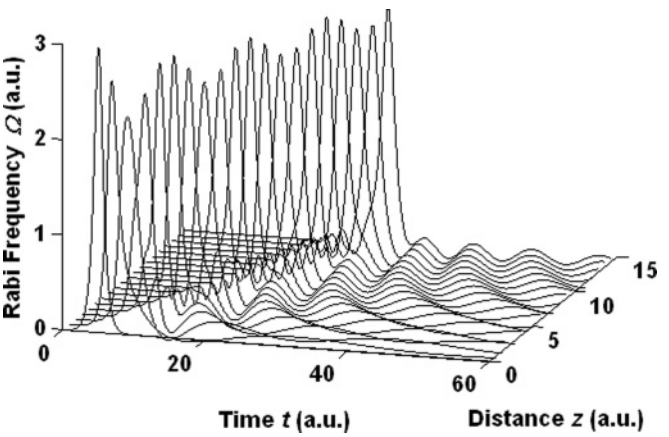

FIG. 6. Evolution of a 1.7π pulse in a homogeneously broadened medium, $\Delta = 0$.

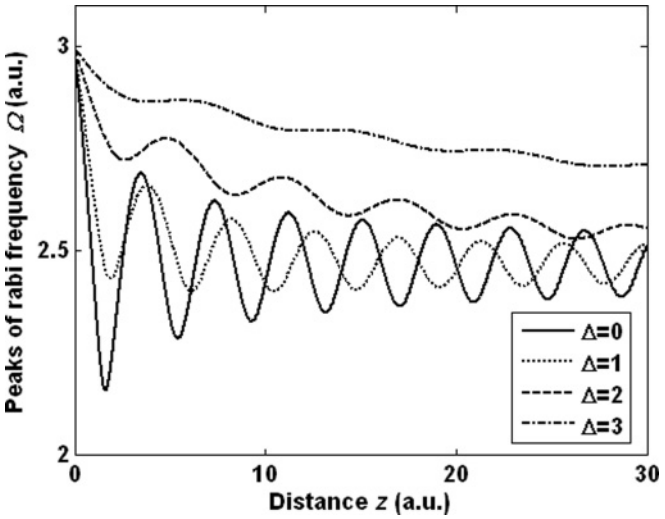

FIG. 7. Evolution of a 1.7π pulse for different detunings in a homogeneously broadened medium.

In previous discussions of area evolution, we ignored both longitudinal and transverse relaxation effects. In general, the longitudinal relaxation time T_1 is far greater than the transverse relaxation time T_2, so the parameter used corresponding to the calculation can be chosen as $T_1 = 10T_2$. Figure 4(a) shows the area evolution of the pulse with $S(0) = 1.7\pi$ as a function of propagation distance for different T_2 in a homogeneously broadened medium. The general picture for each case is similar. For longer propagation distance, the pulse area no longer oscillates around the value 2π and almost deeply decreases to the 0π value. Because of a lack of energy by increasing the value of T_2, the pulse is not able to stabilize and makes itself transform into a 0π pulse. The analysis of Fig. 4(a) indicates that the larger T_2 is, the longer the distance it can propagate is. As to an inhomogeneously broadened medium [see Fig. 4(b)], the evolution form of the pulse area also transforms into a 0π pulse due to the relaxation and energy losses, and the area of the pulse with $T_2 = 10$ does not even reach the 2π value. It is obvious that the collapse curves, from 2π to 0π, are much smoother than the curves under the homogeneous broadening condition. This effect can be explained by the pulse energy loss procedure [7].

The interesting evolution behavior of the pulse area in Fig. 5(a) shows the influence of detuning in a homogeneously broadened medium. In the near-resonant case with $\Delta = 0.1$, the propagation distance before the pulse area approaching to 2π is obviously increased. As the detuning Δ becomes larger, a longer propagation distance under the area value of 1.7π is observed. That means the detuning delays the converting procedure and makes the input pulse more stable at its initial area value, i.e., $\Delta = 0.3$; the pulse oscillates around the value 1.7π for a propagation length of almost 40 (units of $c\tau_0/n$). However, under the inhomogeneous broadening condition, the area evolution of resonant pulse propagation with detuning still mainly obeys the area theorem [see Fig. 5(b)], and the impact is much smaller compared with Fig. 5(a).

We therefore conclude that in atomic media with a decay mechanism, whether the medium has inhomogeneous or homogeneous broadening, the pulse with whatever area value will collapse into 0π. Moreover, in the present studies, for the homogeneous broadening condition, the detuning plays an important role in the evolution of pulse area, but it has relatively little influence on the behavior of area evolution in an inhomogeneously broadened medium.

B. Pulse shape

We now turn to investigating the pulse propagation. The results of the propagation of a 1.7π pulse in a homogeneously broadened medium are presented in Fig. 6. It can be seen that the pulse propagation process is interesting, the pulse shape is obviously deformed, there exists an oscillation tail beside the main pulse, and the peaks of the Rabi frequency are not stable. Combining with the area evolution in Fig. 2(a), we believe that the unstable peaks make the area necessarily oscillate around the value 2π.

Furthermore, we also study the propagation behavior of pulses with other area values, e.g., 1.5π pulse, 1.9π pulse, and 2π pulse. All compared pulses propagate under the same condition. We find that, during the reshaping procedure, the closer the initial pulse area was to 2π, the more stable the Rabi frequency performed (with negligible oscillation tail and more stable peaks).

While considering the influence of detuning (again) on the pulse propagation, we plot the peak curves of the Rabi frequency in Fig. 7. The solid curve, without detuning, presents

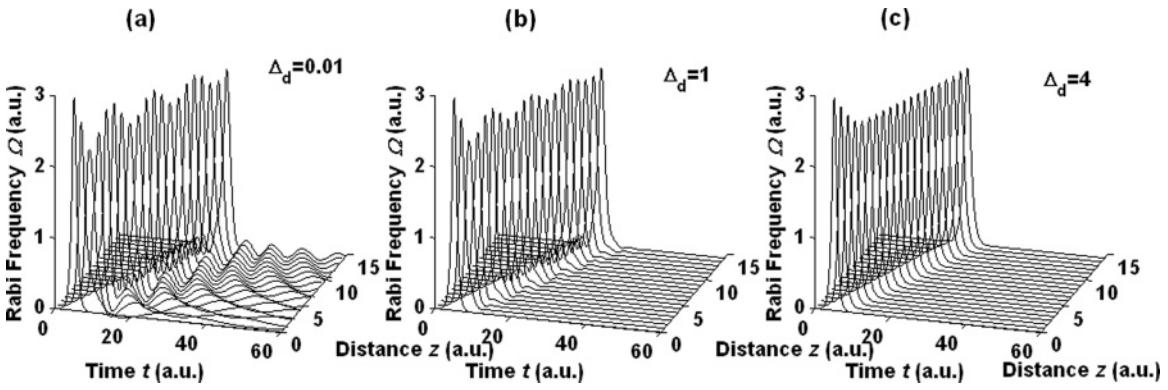

FIG. 8. Evolution of a 1.7π pulse for different FWHM ILS.

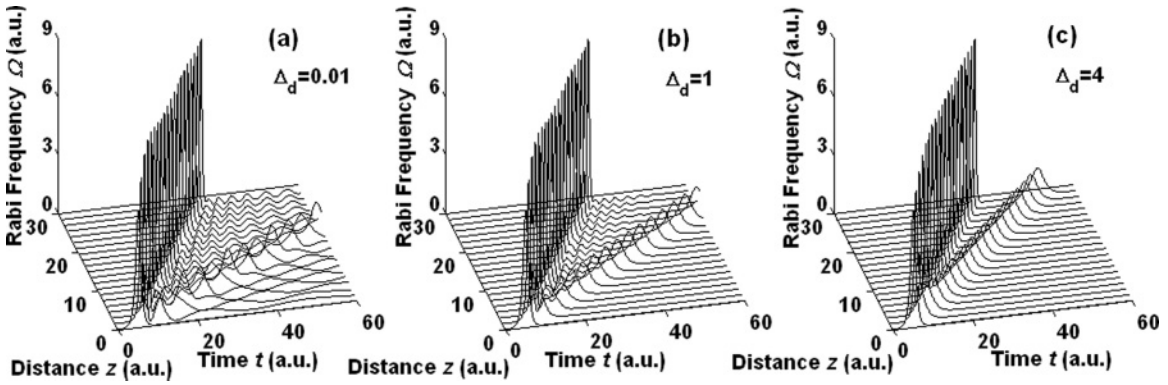

FIG. 9. Evolution of a 3.4π pulse for different FWHM ILS.

a deep decrease after propagating in the medium for a short distance and evolves into an oscillating structure. As to $\Delta = 1$, we observe that the oscillations of peak curves diminished. For the larger detunings (plotted with dash and dash-dotted curves in Fig. 7), the peak value slowly and smoothly decays. Accurately, if we plot the pulse evolution with different detunings in a three-dimensional space time, we will find large detuning slows down the pulse-reshaping process and inhibits the oscillation. Actually, because the spectrum width interaction with atoms in a homogeneously broadened medium is very narrow, a small detuning will hinder the interaction to some extent.

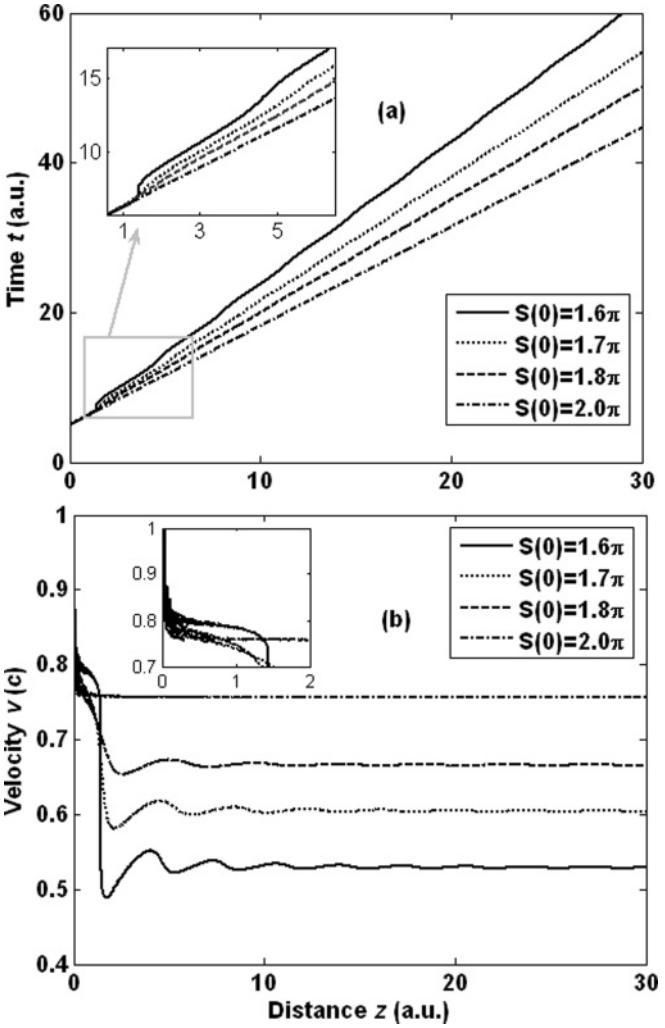

FIG. 10. Evolution of pulse peaks for different input pulse areas in a homogeneously broadened medium. (a) In dimensionless time. (b) In terms of light velocity c.

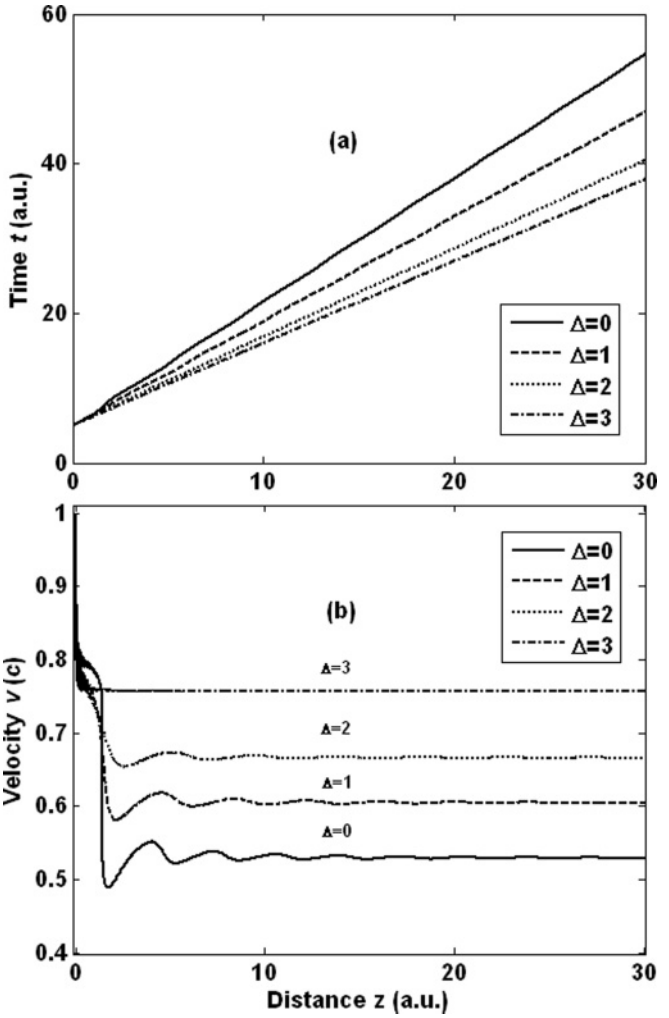

FIG. 11. Evolution of 1.7π-pulse peaks for different detunings in a homogeneous broadened medium. (a) In dimensionless time. (b) In terms of light velocity c.

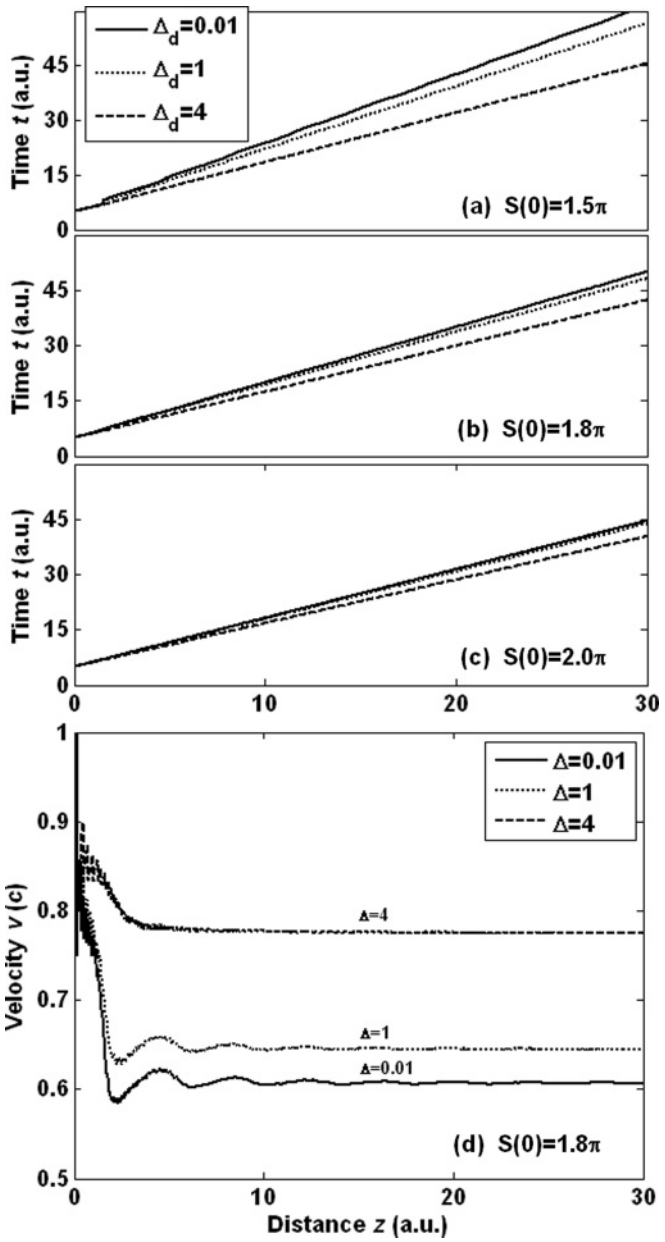

FIG. 12. Evolution of pulse peaks for different FWHM ILS in an inhomogeneously broadened medium. (a), (b), and (c) In dimensionless time. (d) In terms of light velocity c.

As in the inhomogeneously broadened medium, the pulse behaves in a similar way with the performance in Fig. 6; see Fig. 8(a) under slightly FWHM ILS, where we neglect the relaxation and detuning. For the larger detuning plotted in Fig. 8(b), the results suggest that both of the main pulse and oscillation tail transform relatively stably for FWHM ILS $\Delta_d = 1$. Obviously, by increasing the FWHM ILS further such that the pulse-peak reshaping could be obtained in a smooth and slow decrease process, the oscillating structure almost disappeared. Theoretically, for the same incident pulse, the pulse spectrum is fixed, and only the atoms with resonant frequency can have interaction with the pulse. Increasing FWHM ILS means that the rate of active atoms near the central

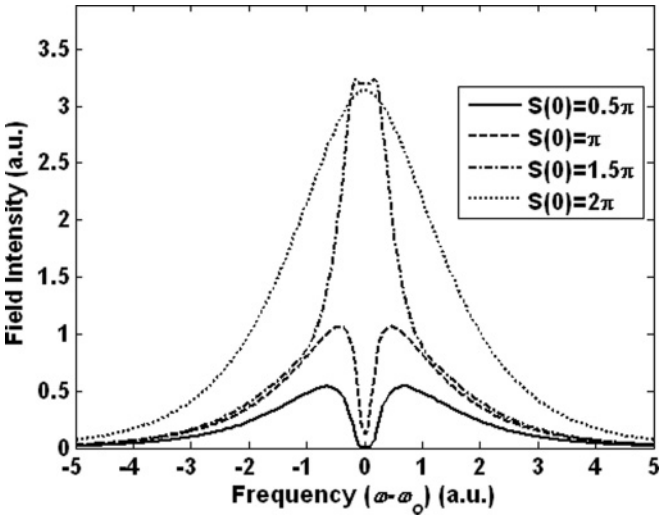

FIG. 13. Spectral shapes of the pulse at z = 1 for different pulse areas in a homogeneous medium.

resonant frequency diminishes. That is the reason why large Δ_d slows the area evolution shown in Fig. 3.

As we know, pulse breakup occurs when the pulses have areas above 3π due to the stimulated absorption and reemission processes [1,21]. The pulse breakup depends on various parameters, including the pulse area, the atomic density, and so on. In Fig. 9 we compare the propagation properties of pulses for different Δ_d. We see that after a small optical path the pulse breakups are observed, the first part sharpens, and the second part widens during propagation. The evolution of the first part is the same as shown in Fig. 8, and the area of the second part is also converted to 2π but with slower velocity and lower energy. When the Δ_d is so small that the pulse breakup in the medium occurs more easily [in Fig. 9(a)] with a relatively short optical path, as for increasing Δ_d, only for a longer optical path will the pulse encounter a sufficient number of atoms to cause reshaping. After the pulse propagates

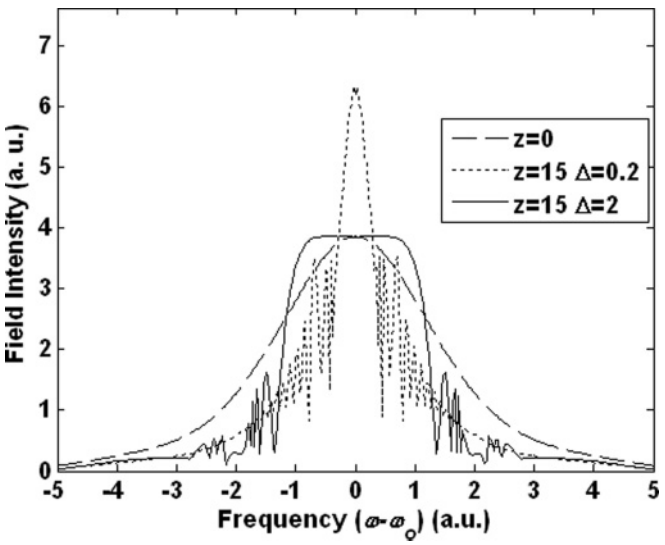

FIG. 14. Spectral shapes of a 1.25π pulse for different detunings in a homogeneous broadened medium; longitudinal time T_1 and transverse time T_2 are both ignored.

TABLE I. Step effects on the maximum global error of methods I, II, and III.

Step h	Analytic solution I	Method I	Error I	Analytic solution II	Method II	Error II	Analytic solution III	Method III	Error III
0.01	2.4847502	2.5244935	0.0397433	2.2538526	3.2770607	1.0231534	2.8965887	2.3250312	0.5715574
0.005	2.5010517	2.4808136	0.0202381	2.4855154	3.0013508	0.5158354	2.7929807	2.5021345	0.2908462
0.001	2.4730871	2.4689348	0.0041523	2.6620791	2.7651681	0.1030890	2.7019673	2.6430887	0.0588786

farther through the medium, we can see the velocities of the second parts are obviously different in the three plots.

Coming to the end of our discussion of the ultrashort pulse propagation, we want to emphasize the propagation relationship between the homogeneous and inhomogeneous broadening. In general, for quite large Δ_d only the central part of the spectrum is active, and the pulse shapes, including both the pulse peaks and with a strong or a weak oscillation tail, also depend mainly on it.

C. Pulse velocity

Another important feature of pulse propagation in a medium is the velocity, which is influenced not only by the pulse properties but also by the optical materials. For an ultrashort pulse, we use the main pulse peaks to mark the pulse trace, and the pulse velocity is reflected according to the corresponding space-time coordinates of the curves.

In the previous sections, we have shown that pulses have a reshaping procedure during their propagation in an absorbing medium, and pulse initial areas have significant influence on the evolutions of the pulse area. Figure 10 presents the evolution of the peaks that reflects the velocity of the pulse. As the optical path is a constant, we find that the pulse with initial area $S(0) = 1.6\pi$ needs the maximum time among the four curves, and the pulse with initial area $S(0) = 1.7\pi$ needs a relatively short propagation time. With the increase of pulse area ($<2\pi$), the needed time becomes shorter and shorter, which means the propagation velocity is increased. A close look at the structure of the four curves shows the following feature: At exactly the early evolution, the trace of the solid curve is not stable, and the velocity of the pulse peak dramatically oscillates. Gradually, the solid curve deviates from the initial direction, and the pulse peak velocity becomes flat, within 0.5–0.8c [22]. Actually, whether the medium has homogeneous or inhomogeneous broadening, the reshaped pulse broadens its width, loses its energy, and slows down.

We also present the numerical study of the detuning effect on the pulse velocity (Fig. 11). If we compare the four curves, we can say roughly that for a pulse without detuning, $\Delta = 0$, the propagation time is the maximum, and for a pulse having detuning $\Delta = 1$ the needed propagation time is shortened. With the further increasing of detuning, the propagation time is pulled toward a limited value. In general, an increase of detuning means the rate of active atoms is diminished, which results in weakening the interaction between the pulse and the medium. Meanwhile, the pulse velocity is naturally increased in the medium but will not exceed the speed of a pulse with an initial area value of 2π.

In this section, we have shown numerically that the pulse velocity in a medium always increases with the greater deviation in pulse-area value from the value of 2π, and we also observe that an increase in detuning or FWHM ILS can cause the pulse velocity to increase. The physical mechanisms are given theoretically.

In Sec. IV A, we studied the influence of Δ_d on area evolution and gave the important results. Furthermore, we investigate the influence of Δ_d on the pulse velocity in our model. Figure 12(a) presents the behavior of pulse peaks with an initial area of 1.5π for various Δ_d. Expectedly, with an increase in Δ_d, the pulse velocity becomes greater because the rate of active atoms near the central resonant frequency diminishes; this statement has been confirmed by the results presented in Figs. 3 and 8. We also illustrate the evolution of pulse with an initial area value of 1.8π for the same Δ_d. Figure 12(b) shows the evolution curves shift toward the direction of smaller time, and the distance between the adjacent curves is also compressed. While the initial area is 2π, the trends mentioned above will be further enhanced. On the other hand, the influence of Δ_d becomes weaker.

D. Pulse spectrum

In this section we discuss the influence of pulse area, detuning, and distance on the spectrum of input pulse. In the case of an inhomogeneous broadened medium, the spectral shapes are similar to a homogeneous broadened medium by averaging atomic variables over a Doppler profile width [16].

In Fig. 13, we plot the spectrum of different pulse areas, propagating in a homogeneous broadened medium with $T_1 =$

TABLE II. Comparison of pulse-area evolution for the numerical solution and the analytic solution. The initial input pulse areas are 1.3π, 1.5π, 1.9π, and 2π.

Error	Pulse area	$z = 3$	$z = 6$	$z = 9$	$z = 12$	$z = 15$
Absolute errors	1.3π	0.0035	0.0012	9.0198×10^{-5}	6.5447×10^{-6}	1.7721×10^{-6}
	1.5π	0.0043	6.2639×10^{-4}	4.5997×10^{-5}	3.3658×10^{-6}	2.5447×10^{-7}
	1.9π	0.0012	8.9803×10^{-5}	6.6600×10^{-6}	5.7334×10^{-7}	1.2950×10^{-7}
Maximum global errors	2.0π	0.0291	0.0290	0.0288	0.0287	0.0278

10, $T_1 = 10T_2$, and $\Delta = 0$. From the discussion of Fig. 4, we choose the small distance of z ($z = 1$), and in this situation the pulse area does not decrease sharply. Frequencies near the atomic frequency show a dip because of the interaction of the dipole field and the pulse.

When detuning is taken into consideration in Fig. 14, the spectral shapes of the pulse evolve into an oscillating structure, especially around resonant frequency. Meanwhile, frequencies near the atomic frequency are amplified. This effect is related to the procedure of light reemission [10,23].

V. CONCLUSIONS

In conclusion, we have presented a predictor-corrector fourth-order Runge-Kutta method for integration of the Maxwell-Bloch equations with partial differential and integral terms. Since the characteristics are used, the Bloch equations only contain a partial derivative with respect to the time-independent variable, thus permitting us to apply the fourth-order Runge-Kutta method; for the Maxwell equation, we choose a middle-grid-point scheme to enhance the calculation accuracy; as to the predictor-corrector method, which effectively improves the accurate results and greatly saves calculation time.

Then, applying the numerical method, we study the evolutions of the pulse area, pulse propagation, and pulse velocity under both homogeneous and inhomogeneous broadening conditions. We prove again that pulse area will collapse to zero under the decay mechanism and find the FWHM ILS and detuning have significant influence on area evolution. The influence under the homogeneous broadening condition is more obvious than in the inhomogeneously broadened medium. As to the pulse-reshaping procedure, we point out that the oscillations of the pulse-peak curve and tail are mainly determined by the value of FWHM ILS and are also affected by detuning. Additionally, we discuss pulse breakup under various FWHM ILS and find pulse velocity changed obviously. In addition, we give the pulse-peak trace that presents the pulse velocity to some extent. For various initial input pulse areas, it shows the pulse velocity becomes greater as the pulse area gets closer to 2π, and a larger detuning also creates greater pulse velocity. As to an inhomogeneously broadened medium for the same medium, a larger FWHM ILS causes the pulse velocity in the medium to be relatively greater. Finally, we discuss the evolution of the pulse spectrum in a homogeneous medium. The spectral shapes demonstrate that with absorption the frequencies near the atomic frequency are absorbed. In the case without consideration of absorption, spectral shapes show an oscillating and complex structure.

ACKNOWLEDGMENTS

This work is supported by the National Natural Science Foundation of China under Grant No. 10574166 and the Guangdong Natural Science Foundation under Grant No. 8151027501000062

I. APPENDIX

We get some other methods in comparison with predictor-corrector fourth-order Runge-Kutta scheme. The part of the Bloch equation adopts Eq. (8), but the part of the Maxwell equation uses different methods.

Method I is a predictor-corrector fourth-order Runge-Kutta method:

$$\Omega_{z+1,t+1} = \Omega_{z,t} + h \cdot (v_{z,t+1} + v_{z+1,t+1})/2. \quad \text{(A1)}$$

Method II is a square mesh of points (see discussion of Eq. (11) in Sec. III),

$$\Omega_{z+1,t+1} = \Omega_{z,t} + h \cdot v_{z,t+1}. \quad \text{(A2)}$$

Method III is a backward difference method,

$$\Omega_{z+1,t+1} = \Omega_{z,t} + h \cdot v_{z,t}. \quad \text{(A3)}$$

We compare numerical solutions by different methods with an analytical solution by hyperbolic-secant pulse at $z = 4$ (units of $c\tau_0/n$), pulse area $S(0) = 2\pi$, detuning $\Delta = 0$, and pulse duration $t_p = 1$ (units of τ_0).

It can be seen from the Table I, in the case of the same step, that the errors of method I are smaller by one or two orders of magnitude than the errors of methods II and III. From the longitudinal view, the step is halved, and errors are half, which means methods II and III, in order to get the same accuracy as method I, must adopt a smaller step and spend more time.

In order to verify the convergence and reliability of the method, we compare the analytical solution of the evolution of pulse area in an inhomogeneous medium with the numerical solution. We adopt a hyperbolic-secant pulse, and laser parameters are as follows: the longitudinal and transverse relaxation times $T_1 = 0$ and $T_2 = 0$, detuning $\Delta = 0$, and step $h = 0.02$. In Table II we get the influence of the propagation distance on the absolute errors of pulse areas, and the results show that with the increase of propagation distance the absolute errors between the numerical solution and the analytical solution get smaller. Also, the maximum global errors of the 2π pulse also get smaller as the distance increases [20]. As mentioned above, it shows the convergence and reliability of the method.

[1] L. Allen and J. H. Eberly, *Optical Resonance and Two-Level Atoms* (Wiley, New York, 1975).
[2] T. Brabec and F. Krausz, Rev. Mod. Phys. **72**, 545 (2000).
[3] M. Hentschel, R. Kienberger, Ch. Spielmann, G. A. Reider, N. Milosevic, T. Brabec, P. Corkum, U. Heinzmann, M. Drescher, and F. Krausz, Nature (London) **414**, 509 (2001).
[4] S. L. McCall and E. L. Hahn, Phys. Rev. Lett. **18**, 908 (1967).
[5] J. Xiao, Z. Wang, and Z. Xu, Phys. Rev. A **65**, 031402 (2002).
[6] J. E. Eberly, Opt. Express **2**, 173 (1998).
[7] A. I. Maimistov, J. Fiutak, and W. Miklaszewski, Z. Phys. B **88**, 349 (1992).

[8] J. E. Rothenberg, D. Grischkowsky, and A. C. Balant, Phys.Rev. Lett. **53**, 552 (1984).
[9] G. S. Vasilev and N. V. Vitanov, Phys. Rev. A **73**, 023416 (2006).
[10] W. Miklaszewski, J. Opt. Soc. Am. B **12**, 1909 (1995).
[11] J. E. Rothenberg and D. Grischkowsky, J. Opt. Soc. Am. B **2**, 626 (1985).
[12] J. E. Rothenberg and D. Grischkowsky, J. Opt. Soc. Am. B **3**, 1235 (1986).
[13] A. Lipsich, S. Barreiro, A. M. Akulshin, and A. Lezama, Phys. Rev. A **61**, 053803 (2000), and references therein.
[14] J. C. Diels and E. L. Hahn, Phys. Rev. A **8**, 1084 (1973).
[15] N. Schupper, H. Friedmann, M. Matusovsky, M. Rosenbluh, and A. D. Wilson-Gordon, J. Opt. Soc. Am. B **16**, 1127 (1999).
[16] J. K. Ranka, R. W. Schirmer, and A. L. Gaeta, Phys. Rev. A **57**, R36 (1998).
[17] J. C. Delagnes, F. A. Hashmi, and M. A. Bouchene, Phys. Rev. A **74**, 053822 (2006).
[18] J. C. Delagnes and M. A. Bouchene, Phys. Rev. A **76**, 023422 (2007).
[19] J. H. Mathews and K. D. Fink, *Numerical Methods Using MATLAB* (Publishing House of Electronics Industry, Beijing, 2005).
[20] L. Cheng, Z. Huarong, and Y. Xiangyang, Acta Sci. Nat. Univ. Sunyatseni **48**, 36 (2009).
[21] W. Miklaszewski and J. Fiutak, Z. Phys. B **93**, 491 (1994).
[22] D. Grischkowsky, E. Courtens, and J. A. Armstrong. Phys. Rev. Lett. **31**, 422 (1973).
[23] J. C. Delagnes and M. A. Bouchene, Phys. Rev. A **76**, 023422 (2007).